

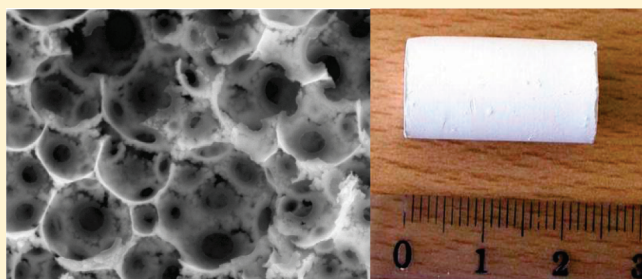
# Preparation, Solid-State NMR, and Physicochemical Characterization of Surprisingly Tough Open Cell PolyHIPEs Derived from 1-Vinyl-1,2,4-triazole Oil-in-Water Emulsions

Fabrice Audouin,<sup>†</sup> Marc Birot,<sup>†</sup> Éric Pasquinet,<sup>‡</sup> Olivier Besnard,<sup>‡</sup> Pascal Palmas,<sup>\*,‡</sup> Didier Poullain,<sup>‡</sup> and Hervé Deleuze<sup>\*,†</sup>

<sup>†</sup>Institut des Sciences Moléculaires, CNRS-UMR 5255, Université de Bordeaux, 351 cours de la Libération, F-33405 Talence, France

<sup>‡</sup>CEA, DAM, Le Ripault, F-37260, Monts, France

**ABSTRACT:** Interconnected microcellular polymeric monoliths have been prepared from oil-in-water concentrated emulsions of aqueous 1-vinyl-1,2,4-triazole using the high internal phase emulsion methodology. The polyHIPE materials thus obtained present a typical polyHIPE morphology having unexpectedly high mechanical strengths considering their low cross-linking level (3 mol % of *N,N'*-methylenebis(acrylamide)). <sup>13</sup>C, <sup>15</sup>N, and <sup>1</sup>H solid-state NMR analyses confirm the expected polymer structure and evidenced the presence of polymer chain association by strong hydrogen bonding with water.



## INTRODUCTION

Among polyvinylazoles, polymers and copolymers based on 1-vinyl-1,2,4-triazole (VT) are of particular interest due to their unique properties (i.e., nontoxicity, high hydrophilicity, chemical stability, complexing power, heat resistance) and show promise for the food industry as well as for engineering and energetic materials.<sup>1</sup> Poly(VT) can be synthesized in good yields by free radical polymerization in polar solvents.<sup>2</sup> VT has been copolymerized with various monomers such as styrene and methyl methacrylate<sup>3</sup> and, more recently, with 2-hydroxyethyl methacrylate.<sup>4</sup> In each case, VT appeared to be less reactive than its comonomer—a behavior that has been attributed to the polarization of the vinyl group under the influence of the azolyl substituent.

Concerning the complexing power of poly(VT) derivatives, VT was copolymerized with acrylamide, and the obtained copolymers were used for flocculation studies of kaolin suspensions after azole ring quaternization.<sup>5</sup> Poly(ethylene glycol dimethacrylate)-*co*-VT beads were prepared by radical copolymerization of the corresponding monomers in suspension polymerization. The adsorption capacity of the obtained beads for Cd(II), Hg(II), and Pb(II) in aqueous media was investigated.<sup>6</sup> Finally, very recently, copolymers of VT cross-linked with divinyl sulfide or divinyl diethylene glycol ether were prepared as mercury sorbents,<sup>7</sup> whereas energetic polymer salts were synthesized by protonation of poly(VT) with inorganic or organic salts.<sup>8</sup>

Emulsion templating is a simple and versatile method for the preparation of microcellular materials (cell size range 2–100  $\mu\text{m}$ ) by polymerizing the continuous phase of a high internal phase emulsion (HIPE). The obtained materials have been called polyHIPEs by Unilever researchers.<sup>9</sup> Theoretically, the final solid

polymer is expected to have an open-cell morphology only for a sufficiently concentrated HIPE (dispersed phase volume fraction >74% of the total emulsion).<sup>10</sup> Nevertheless, such a structure has been observed for lower values.<sup>11</sup> The historical polyHIPE preparation involves the formation of a stable, water-in-oil concentrated emulsion using hydrophobic monomers as part of the continuous phase (most generally a mixture of styrene and divinylbenzene with, optionally, the addition of a functionalized styrene such as 4-vinylbenzyl chloride) and an aqueous phase as the dispersed phase.

A great deal of work by a continuously increasing number of researchers has been devoted to the study of this particular system.<sup>12–18</sup> The main topics studied have been the control of the porous morphology (size dispersion of cells and interconnecting windows)<sup>19–24</sup> and attempts to increase the mechanical strength of the material, which in its native formulation is generally considered insufficient for practical applications.<sup>25–28</sup> Several efforts have also been devoted to the use of hydrophobic (meth)acrylate derivatives.<sup>29,30</sup>

Much less work has been published on the synthesis of polyHIPEs based on hydrophilic (i.e., water-soluble) monomers emulsified by a hydrocarbon. Krajnc and co-workers reported on the preparation of a so-called “reverse” polyHIPE by polymerization of an oil-in-water HIPE consisting of an aqueous mixture of acrylic acid and *N,N'*-methylenebis(acrylamide) (MBA) as the continuous phase and toluene as the dispersed phase.<sup>31</sup> Superabsorbents have been prepared using a similar

**Received:** April 14, 2011

**Revised:** May 23, 2011

**Published:** May 27, 2011

approach.<sup>32</sup> Concomitantly, Barbetta and co-workers prepared gelatin— and dextran—methacrylate polyHIPE scaffolds through a direct concentrated emulsion.<sup>33,34</sup>

The use of heterocyclic vinyl monomers for the preparation of polyHIPEs materials has hardly been studied at all. Maleimide and bismaleimide monomers have been copolymerized with styrene in concentrated reverse emulsions to give polyHIPEs with an increased thermal resistance.<sup>35</sup> Poly(aryl ether sulfone) polyHIPE materials have been synthesized by copolymerizing a maleimide-terminated aryl ether sulfone macromonomer with styrene and divinylbenzene in a nonaqueous HIPE.<sup>36</sup>

During the course of our research on the development of new kind of porous polymers using the emulsion-templated approach,<sup>37</sup> we recently reported on the potential of 1-vinyl-5-aminotetrazole to give a tough polyHIPE material from direct emulsion using only low amounts of cross-linking agent.<sup>38</sup> However, this material presented the drawback of requiring the synthesis of the monomer. We thus now present the results obtained when using the commercially available 1-vinyl-1,2,4-triazole to give hydrophilic, self-standing monoliths for potentially interesting applications such as supports for heterogeneous catalysts or metal complexing devices.<sup>39</sup>

## EXPERIMENTAL SECTION

**Materials.** 1-Vinyl-1,2,4-triazole (VT) and benzoyl peroxide (BPO) were purchased from Fluka; *N,N'*-methylenebis(acrylamide) (MBA) and dodecane were obtained from Acros Organics. 2,2'-Azobis(2-methylpropionamide) dihydrochloride (V50) was purchased from Wako Chemicals, GmbH. Potassium persulfate  $K_2S_2O_8$  (99%+, ACS reagent), Igepal CO-890, Tween 20, and Tween 80 were obtained from Aldrich. All these chemicals were used as received.

**Bulk Polymerization.** VT (600 mg, 6.3 mmol) and MBA (32.6 mg, 0.21 mmol) were mixed with potassium persulfate (6 mg) and heated at 60 °C for 24 h under a flow of nitrogen. The precipitate was filtered, washed with ethanol, and dried under vacuum to constant weight (504 mg, yield = 76%).

**HIPE Preparation.** In a typical experiment, VT (6 g), Igepal CO-890 (1.5 g), Brij 98 (1.5 g), MBA (0.3 g), double-distilled water (6 g), and potassium persulfate (0.3 g) were placed in a test tube. The mixture was homogenized at room temperature through sonication. Emulsification was performed using a laboratory-made system already described elsewhere.<sup>40</sup> Briefly, this device is composed of two polypropylene syringes (50 mL, internal diameter (i.d.) = 28 mm) connected with a small-section tube (i.d. = 4 mm,  $L$  = 20 mm). The aqueous components of the emulsion (about 20 mL) were put into one of the syringes, and dodecane (10 g) was added. A second syringe was connected to the first one using the small connecting tube. This system was then adjusted in the “two-syringe” emulsification device, and the emulsion was formed by successive passages through the tube produced by the backward and forward motion of the syringe plungers. The rate of passage of the emulsion through the connecting tube was adjusted to 7 min<sup>-1</sup>. The emulsification time was 25 min.

**PolyHIPE Preparation.** The obtained thick white emulsion was placed in tightly closed PTFE cylindrical molds of varying sizes and was polymerized for 24 h at 60 °C in an oven. The resultant polyHIPE monoliths were extracted by successively refluxing with ethanol and acetone (24 h each) in a Soxhlet apparatus. Drying was then performed in a vacuum oven at room temperature to constant weight.

**Characterization of the Monoliths.** *Solid-State NMR Measurements.* All experiments were carried out at room temperature on a Bruker Avance 400 MHz spectrometer using broadband X-H CP/MAS probes with sizes of 7 mm (for <sup>13</sup>C) and 4 mm (for <sup>15</sup>N and <sup>1</sup>H) external

diameter rotors. The polyHIPE monolith was first ground into a thin powder, packed down in the MAS rotors, and analyzed with the cross-polarization procedure (CP) under magic angle spinning (MAS). <sup>13</sup>C spectra were recorded at a spinning frequency  $\nu_r$  = 6 kHz using a standard linear ramped amplitude (50–100%). An average nutation frequency  $\nu_H$  = 43 kHz was applied during the 1 ms CP period on the <sup>1</sup>H channel at the first sideband in the matching Hartmann–Hahn profile ( $n$  = -1). For the hard excitation pulse,  $\nu_H$  was adjusted to 80 kHz. For the <sup>15</sup>N experiments, another optimized sequence was performed to compensate for the MAS modulation of the Hartmann–Hahn CP profile.  $\nu_H$  was set to 65 kHz during the CP period and to 100 kHz for the hard pulse. This sequence contained a tangential pulse applied on the X channel during the CP which produces an adiabatic passage through the Hartmann–Hahn condition  $n$  = -1.<sup>41</sup> Details concerning this experiment and its optimization for the <sup>1</sup>H–<sup>15</sup>N CP transfer are beyond the scope of the present article and will be provided elsewhere. The shaped amplitude was here calculated assuming a <sup>1</sup>H–<sup>15</sup>N dipolar coupling of 5 kHz. Spectra were recorded with a contact time  $t_{CP}$  = 2 ms at a spinning frequency  $\nu_r$  = 15 kHz. <sup>1</sup>H spectra were acquired at the same MAS frequency following two excitation schemes: (i) a simple 90° flip angle pulse to detect the whole proton spectrum and (ii) a CPMG (Carr–Purcell–Meiboom–Gill) pulse train applied prior to the acquisition and synchronized with sample MAS rotation. The pulse train corresponded to a succession of  $n$  cycles composed of a 180° refocusing pulse flanked at both sides by a delay of 133  $\mu$ s that corresponds to two rotor periods. The sequence acted as a  $T_2$  relaxation filter eliminating the large <sup>1</sup>H components of the backbone from the spectrum. Only the narrow lines remained, corresponding to the more mobile fraction of the molecular system, i.e., small solvent molecules or flexible polymer moieties. The benefit of this sequence, in comparison with a standard Hahn echo, is the compensation of 180° pulse imperfections and a reduction of the effect of diffusion that can affect the intensity measured for small molecules.

For the sake of efficiency, the corresponding  $T_2$  relaxation time needed to be large in comparison with the total relaxation delay. For the purpose of quantitative analysis,  $T_2$  relaxation times were measured with the two-dimensional version of the CPMG sequence using 128 relaxation delay increments between 133  $\mu$ s and 17 ms. <sup>1</sup>H, <sup>13</sup>C, and <sup>15</sup>N chemical shifts were calibrated according to external secondary references: water (4.8 ppm with respect to TMS, 0 ppm), adamantane (upfield <sup>13</sup>C transition at 38.46 ppm in regard to TMS, 0 ppm), and NH<sub>4</sub>NO<sub>3</sub> (downfield transition at -358.4 ppm with respect to CH<sub>3</sub>NO<sub>2</sub>, 0 ppm).

**Porosity Determination.** The effective porosity and the connection size distribution of each sample were determined by mercury intrusion porosimetry using a Micromeritics Autopore IV 9500 porosimeter. The reported average connection size corresponded to the median pore diameter by volume.

**Specific Surface Area and Mesoporosity Determination.** The specific surface area was determined by N<sub>2</sub> adsorption measurements performed on a Micromeritics ASAP 2010. The collected data were subjected to the Brunauer, Emmett, and Teller (BET) method.<sup>42</sup>

**Electron Microscopy Investigations.** The morphology of the monoliths was observed by scanning electron microscopy (SEM) in a Hitachi TM-1000 microscope. Micrographs were taken at several magnifications between  $\times 1000$  and  $\times 10\,000$ . Pieces of the polyHIPEs (sections of about 0.5 cm<sup>2</sup>) cut from the corresponding monoliths were mounted on a carbon tab, which ensured a good conductivity. A thin layer of gold was sputtered on the polyHIPE fragments prior to analysis. An average cell diameter was estimated for some samples from the SEM micrographs after image processing with Scion Image freeware (Scion Corp., Frederick, MA). The mean and the standard deviation were drawn by manual measurements of diameters from a population of at least 50 cells. To obtain a better estimation of the real cell diameter, a statistical

**Table 1. Formulation of VT-MBA Emulsions Using Different Surfactants**

sample	surfactant (HLB)	surfactant (mg)	H <sub>2</sub> O (mg)	dodecane (g)	emulsion stability
E1VT	T1 <sup>a</sup> (16.7)	80	200	1.6	++
E2VT	T2 <sup>b</sup> (15.0)	80	200	1.6	–
E3VT	T3 <sup>c</sup> (15.3)	80	200	1.6	++
E4VT	T4 <sup>d</sup> (17.8)	80	200	1.6	++
E34VT1	T3 + T4	40 + 40	200	1.6	+++

<sup>a</sup> T1 = Tween 20. <sup>b</sup> T2 = Tween 80. <sup>c</sup> T3 = Brij 98. <sup>d</sup> T4 = Igepal CO-890. In all experiments, the VT (200 mg) and MBA (10 mg) amounts were kept constant.

correction was introduced by multiplying the observed average value by a factor  $K = 2/(3^{1/2})$ .<sup>23</sup>

**Mechanical Analysis.** Compression tests were carried out by the Pôle Européen de Plasturgie (Oyonnax, France) at room temperature on a Zwick 1455 dynamometer with a loading cell of 200 N. Cylindrical samples (diameter = 8 mm, thickness = 10 mm) were compressed at a constant rate (1 mm min<sup>−1</sup>) on their flat surfaces. The mean value and the standard deviation of the Young modulus  $E$  were calculated from the data obtained for five samples of the same composition.

**Thermogravimetric Analysis (TGA).** Weight loss studies of the monoliths were performed on a Netzsch STA 409 under N<sub>2</sub> argon atmosphere. The heating rate was 10 °C min<sup>−1</sup>, and the temperature ranged from 25 to 1000 °C.

**Elemental Analysis.** Elemental analyses were performed by the Service Central d'Analyses (Vernaison, France).

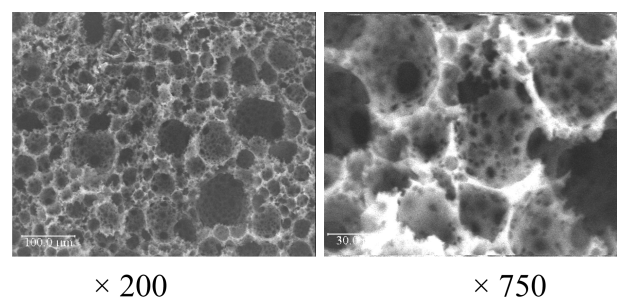
## RESULTS AND DISCUSSION

Since VT was much more soluble in water than in hydrocarbons, the emulsion to be prepared was of the oil-in-water type. Therefore, the cross-linking agent had to be soluble in water. The commercially available *N,N'*-methylenebis(acrylamide) (MBA) was selected as a suitable agent.

In order to facilitate the reading, a labeling code was established for each sample prepared in this work: the first character of a sample name indicates its status: E for HIPE and P for polyHIPE. The following numbers indicate the nature of the surfactant used; VT is for 1-vinyl-1,2,4-triazole. Finally, the last digit is for samples classification. For example, E34VT1 is the first HIPE prepared with a mixture of T3 and T4 surfactants.

**Study of the Bulk Copolymerization of VT with MBA.** As a first approach, it was necessary to verify the bulk radical copolymerization ability of VT and MBA. Radical copolymerization of the mixture of VT with MBA (molar fraction 3%) was conducted in the bulk at 60 °C using potassium persulfate as the initiator. An insoluble polymer was obtained with a satisfactory yield (76%).

**Formulation of a Stable VT-MBA Oil-in-Water HIPE and PolyHIPE Preparation.** Since both monomers were water-soluble, the dispersed phase of the direct concentrated emulsion had to be a hydrocarbon such as dodecane. The choice of the surfactant was crucial for the formation and stability of the emulsion. Several nonionic surfactants with a HLB value between 15 and 20 (generally employed for direct emulsion fabrication) were tested in order to obtain stable VT-MBA emulsions. The various surfactants used were polyoxyethylene (20) sorbitan monolaurate (Tween 20, T1), polyoxyethylene (20) sorbitan monooleate (Tween 80, T2), polyoxyethylene (20) oleyl ether (Brij 98, T3), and polyoxyethylene (40) nonylphenyl ether

**Figure 1.** SEM micrographs of the P34VT1 monolith sample.

(Igepal CO-890, T4). Preliminary experiments showed that VT could not be emulsified in the bulk with a hydrocarbon, regardless of the surfactant (among the above) used. Therefore, for the remainder of the work, the continuous phase was an aqueous solution of the comonomers (mass fraction ~50%). The results of the different formulations tested are reported in Table 1.

The stability of the emulsions was appreciated by visually observing whether any creaming took place after 24 h at room temperature. The use of only one surfactant gave encouraging but insufficient results in terms of emulsion stability only for Brij 98 (E3VT) and Igepal CO-890 (E4VT). Finally, a mixture of T3 and T4 (50:50 wt %) gave emulsions with a good stability and without creaming over a week of storage at room temperature. Therefore, this mixture of surfactants was selected for the work that followed.

Sample E34VT1 was heated to 50 °C for 24 h in order to achieve radical polymerization. The obtained monolith (P34VT1) was washed with water and then ethanol and finally dried at 60 °C under vacuum for several days (yield = 85%).

**Microstructure.** SEM analysis revealed that the P34VT1 sample possessed the characteristic interconnected macroporous structure of polyHIPE materials, that is, microsized spherical voids corresponding of the internal phase droplets imprint interconnected by small circular pores (or interconnections) (Figure 1).<sup>12</sup>

The total porosity of the polyHIPE materials,  $\phi_{\text{total}}$ , can be identified with the expected porosity, assuming the complete removal of all the nonpolymerizable components of the emulsion (dispersed phase, water, and surfactant) and in the absence of any shrinking of the monolith during washing and drying.  $\phi_{\text{total}}$  was calculated with the assumption that all the constituents of the emulsion had a density equal to that of water.  $\phi_{\text{exp}}$  represents the experimental porosity of the material as estimated by mercury intrusion analysis.

In the case of sample P34VT1, the expected porosity was  $\phi_{\text{total}} = 82\%$ , whereas the experimental value was  $\phi_{\text{exp}} = 79\%$ . The difference observed may be due to the volume shrinkage of the monolith during the washing and drying steps. The average connection size estimated by mercury intrusion porosimetry was 2.6  $\mu\text{m}$ , with a broad distribution.

**Influence of the Emulsification Conditions.** The previous experiment was conducted using a vortex as the emulsification system. This apparatus is limited to milligram-scale emulsion preparation. To prepare samples on a multigram scale, other types of emulsifiers were required.

We have recently developed a laboratory-scale emulsification system, called the “two-syringe” emulsification device, specially designed for the preparation of HIPEs.<sup>40</sup> Two VT-MBA concentrated emulsions with different internal phase ratio ( $\phi_{\text{disp}}$ ) were prepared using this technique (Table 2).



**Table 2. Preparation of VT-MBA HIPEs Using the “Two Syringes” Emulsification Device**

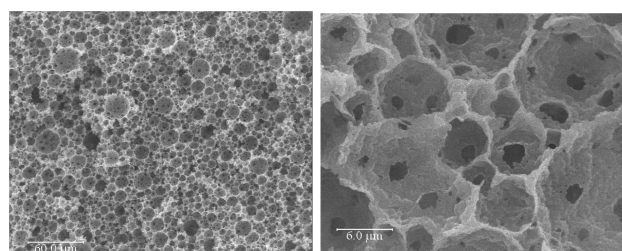
emulsion <sup>a</sup>	dodecane (g)	$\phi_{\text{disp}}^b$ (%)
E34VT2	24	82.0
E34VT3	10	75.0

<sup>a</sup> Continuous phase composition: VT (6 g), MBA (0.3 g),  $\text{K}_2\text{S}_2\text{O}_8$  (0.3 g), T3 + T4 (1.5 g + 1.5 g), water (6 g). <sup>b</sup> Emulsion dispersed phase ratio.

**Table 3. Characteristics of VT-MBA PolyHIPEs Prepared Using the “Two Syringes” Emulsification Device**

polymer	$\phi_{\text{total}}^a$ (%)	$\phi_{\text{exp}}^b$ (%)	av connection size ( $\mu\text{m}$ )
P34VT2	82	81	1.6
P34VT3	75	69	0.6

<sup>a</sup> Porosity expected from the volume fraction of dispersed phase in the emulsion. <sup>b</sup> Experimental porosity estimated by mercury porosimetry. <sup>c</sup> Estimated by mercury porosimetry.



× 350

× 3500

**Figure 2.** SEM micrographs of the P34VT3 sample.

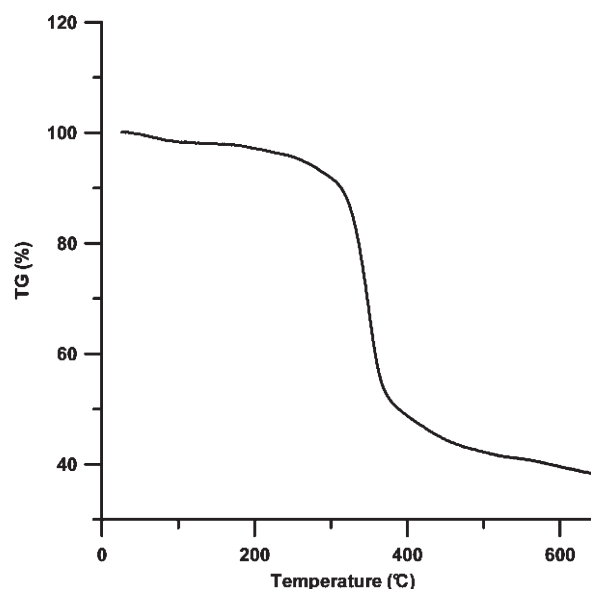
The obtained corresponding HIPEs were put into PTFE molds and heated at 60 °C for 24 h in order for them to polymerize. After solvent extraction and drying, the porosity of the obtained monolith was estimated by mercury intrusion porosimetry (Table 3). In both cases,  $\phi_{\text{exp}}$  was rather close to the expected value  $\phi_{\text{total}}$ .

SEM analysis revealed that samples possessed the characteristic interconnected microcellular morphology of polyHIPE materials (Figure 2 for P34VT3). The cell size distribution was less broad than in the case of the vortex emulsification system.

**Specific Surface Area.** The specific surface area (BET) value of sample P34VT3 was estimated to  $S_{\text{BET}} = 3 \text{ m}^2 \text{ g}^{-1}$ . This value was in accordance with those obtained for styrene/divinylbenzene polyHIPE materials of similar structure.<sup>43</sup>

**Thermal Analysis.** The thermal degradation of the VT-MBA polyHIPE monoliths was examined by TGA. Since these materials were hygroscopic, the samples were dried under vacuum at 100 °C and stored in a desiccator before analysis. Figure 3 shows the thermogram obtained for sample P34VT3 by heating under argon from 40 to 600 °C. A mass fraction loss of 2%, attributed to the removal of bound water, was observed around 100 °C, followed by an important weight loss beginning around 340 °C. The final weight loss at 600 °C corresponded to about 60%. This behavior was in agreement with data reported for the poly(1-vinyl-1,2,4-triazole) homopolymer.<sup>44,45</sup>

**Preparation of Large-Size VT-MBA PolyHIPE Monoliths.** Large-size VT-MBA polyHIPE monoliths were prepared for CEA

**Figure 3.** TGA analysis of sample P34VT3.**Table 4. Formulations of Large-Size VT-MBA HIPEs**

emulsion <sup>a</sup>	dodecane (g)	$\phi_{\text{disp}}^b$ (%)
P34VT4	40	84.1
P34VT5	60	87.7
P34VT6	80	90.0

<sup>a</sup> Continuous phase composition: VT (10 g), MBA (0.5 g),  $\text{K}_2\text{S}_2\text{O}_8$  (0.4 g), T3 + T4 (2.4 g + 2.4 g), water (10 g). <sup>b</sup> Emulsion dispersed phase ratio.

specific applications. Sizes and characteristics of some of them are reported in the following. Formulations of the employed HIPEs are the same as used for previously. The amount of dispersed phase (dodecane) and the corresponding expected internal phase ration of the obtained emulsions are reported in Table 4.

Table 5 lists the shrinkage with regard to the diameter  $D$ , length  $L$ , and total volume of the VT-MBA polyHIPE monoliths. According to this data, the shrinkage was rather limited and very similar regardless of the amount of dodecane used for the emulsion preparation.

SEM analysis confirmed that the samples possessed the characteristic open microcellular structure of polyHIPE materials (Figure 4 for sample P34VT4).

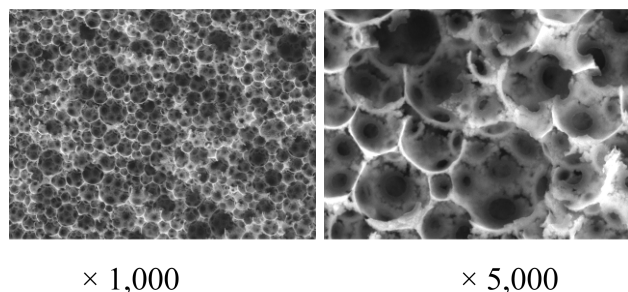
**Porosity Analysis.** Porosity characteristics and specific surface area were determined for the different samples prepared. Data are reported in Table 6.

Experimental porosities ( $\phi_{\text{exp}}$ ) of all samples were close to the expected values ( $\phi_{\text{total}}$ ), confirming the low volume shrinkage of the monoliths during the washing and drying steps. The average voids and connections diameters are in the range of those of already reported for “reverse” polyHIPEs materials<sup>31</sup> and appear to be independent of the total porosity of the sample. The specific surface area values obtained are rather low and attest to the nonporogenic behavior of water in that case.<sup>23,24</sup>

Voids are the solid imprint of the dispersed phase droplets of the concentrated emulsion used as template. Therefore, their size distribution reflects directly the droplets size distribution of the

**Table 5.** Shrinking of Large-Size VT-MBA PolyHIPE Monoliths

polymer	PT34VT4	PT34VT5	PT34VT6
PTFE mold's internal dimensions (mm)	$D = 30, L = 50$	$D = 30, L = 50$	$D = 30, L = 50$
monolith dimensions after washing and drying (mm)	$D = 26, L = 46$	$D = 26, L = 45$	$D = 26, L = 44$
shrinkage of diameter (%)	13	13	13
shrinkage of length (%)	8	10	12
shrinkage of volume (%)	31	32	33

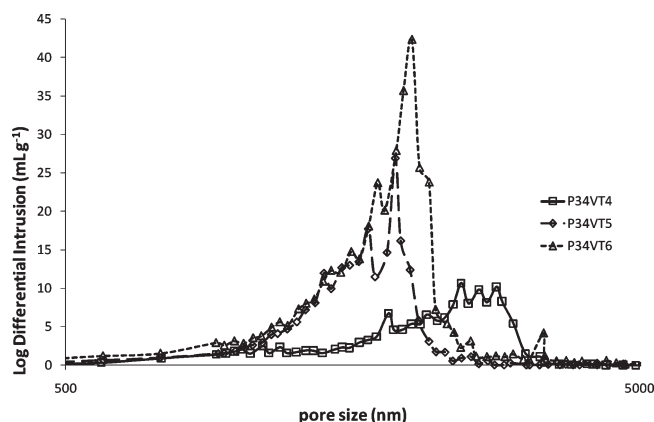
**Figure 4.** SEM micrographs of the P34VT4 sample.

original emulsion. Then, it is possible to calculate the uniformity factor ( $U$ ) using the following relations:  $d^* = (\sum n_i d_i^4 / \sum n_i d_i^3)^{1/3}$  and  $U = (1/d^*) \times (\sum |d^* - d_i| \times n_i d_i^3 / \sum n_i d_i^3)$ , where  $n_i$  is the number of droplets of diameter  $d_i$  and  $d^*$  is the median diameter (the diameter for which the cumulative undersize volume fraction is equal to 0.5).<sup>46</sup> The  $U$  data reported in Table 6 indicate that the voids distribution of VT-MBA polyHIPEs samples prepared are close from the value generally accepted for a monodisperse emulsion ( $U < 0.25$ ).<sup>47</sup>

The ratio  $d/D$  provides information about the structure of the emulsion before gelation.<sup>23</sup> Results for large-size VT-MBA samples are reported in Table 6, the relatively low values obtained reflect the good stability of the emulsion and the rather low porosity of the material prepared.

The interconnect distribution curves are similar for P34VT5 and P34VT6 samples and P34VT4 sample having a higher average interconnect diameter (Figure 5). However, the average connection sizes are quite similar (Table 6).

**Compressive Strength Analysis.** Stress–strain analysis in compression mode was conducted at room temperature for some of the samples. In open-cell foams, the relative Young modulus (foam modulus  $E^*$ , divided by bulk material modulus  $E_b$ ) can be related to the square of the relative density (foam density  $d^*$ , divided by bulk density  $d_b$ ) according to the relation  $E^*/E_b = C(d^*/d_b)^2$ ,  $C$  being a constant of proportionality. In the case of open cell materials, the value of  $C$  is usually taken to 1.<sup>48</sup> An analysis of a nonporous bulk monolith of VT-MBA copolymer gives values of around  $1.34 \text{ g cm}^{-3}$  for the bulk density (foam wall density) and of  $741 \pm 23 \text{ MPa}$  for the Young modulus. An estimate of the foam density of the foams can therefore be calculated for each monolith prepared. The corresponding values are listed in Table 6 (foam density). These values can be compared with those obtained from mercury intrusion/extrusion data (apparent density) also reported in Table 6. A rather good accordance between both approaches can be observed for all samples.

**Figure 5.** Interconnect pore size distribution of VT-MBA polyHIPE materials.**Table 6.** Porosity Characteristics and Stress–Strain Analysis of VT-MBA PolyHIPE Monoliths

sample	P34VT4	P34VT5	P34VT6
$\phi_{\text{total}}^a$ (%)	84.1	87.7	90.0
$\phi_{\text{exp}}^b$ (%)	$78.2 \pm 0.1$	$81.2 \pm 0.1$	$86.9 \pm 0.1$
specific surface area (BET) ( $\text{m}^2 \text{ g}^{-1}$ )	$3.10 \pm 0.02$	$3.00 \pm 0.03$	$2.90 \pm 0.03$
av connection size <sup>c</sup> ( $\mu\text{m}$ ): $d$	$1.9 \pm 0.1$	$1.8 \pm 0.1$	$1.8 \pm 0.1$
av void size <sup>d</sup> ( $\mu\text{m}$ ): $D$	$6.2 \pm 0.6$	$7.4 \pm 0.6$	$7.5 \pm 0.5$
$d/D$	0.31	0.24	0.24
$U$ factor <sup>e</sup>	0.22	0.35	0.22
Young's modulus (MPa)	$54.8 \pm 10.5$	$33.6 \pm 6.6$	$20.9 \pm 4.6$
foam density <sup>e</sup> ( $\text{g mL}^{-1}$ )	0.36	0.28	0.22
apparent density <sup>e</sup> ( $\text{g mL}^{-1}$ )	0.29	0.22	0.14

<sup>a</sup> Porosity expected from the volume fraction of dispersed phase in the emulsion. <sup>b</sup> Experimental porosity estimated by mercury porosimetry.

<sup>c</sup> Estimated by mercury porosimetry. <sup>d</sup> Estimated from SEM micrographs. <sup>e</sup> See text for determination.

The obtained compressive Young modulus values for VT-MBA polyHIPEs are also reported in Table 6. These values appear to be very high for polyHIPE materials, especially considering the expected cross-linking level which amounts to only 3.1%. As an example, a styrene/divinylbenzene (1:1 w/w) polyHIPE prepared under similar conditions with 83% porosity gave a compressive modulus of  $25.0 \text{ MPa}$ .<sup>40</sup> However, these values are very similar to those recently reported for polyHIPE materials prepared using the closely related 1-vinyl-5-amino-tetrazole.<sup>39</sup>

The unexpectedly high mechanical strength for the polyHIPE materials prepared in this work with a rather low cross-linking

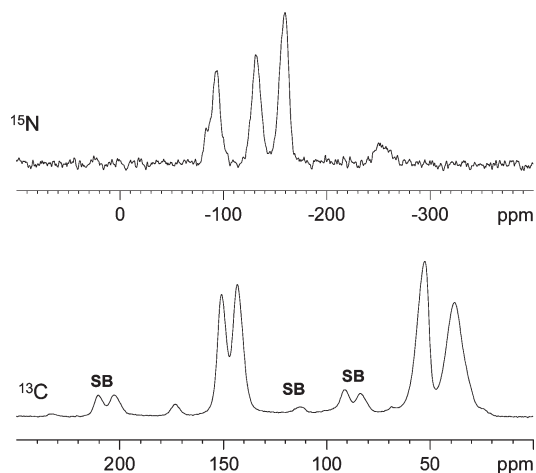


**Figure 6.**  $^{13}\text{C}$  ramp- and  $^{15}\text{N}$  adiabatic-CP/MAS NMR spectra obtained at MAS frequencies of 6 and 15 kHz, respectively. SB stands for spinning sideband.

level could be explained by the specific properties of the principal monomer used that formed high level hydrogen bonds with water molecules. These bonds may generate strong interactions between polymeric chains, increasing their mechanical strength. In order to assess fully this hypothesis, we decided to conduct an in-depth solid-state NMR analysis of a sample of VT-MBA polyHIPE.

**Structural Characterization by Solid-State NMR.** Solid-state NMR is a powerful tool for structural determination of cross-linked polymers. However, surprisingly, it appears to have been scarcely used for polyHIPE analysis.<sup>24,49,50</sup> We investigated the chemical structure of the VT-MBA polyHIPE monoliths by MAS NMR spectroscopy (on sample P34VT4). In addition with the more common  $^1\text{H}$  and  $^{13}\text{C}$  MAS NMR analysis,  $^{15}\text{N}$  MAS NMR spectra were also recorded as previously reported for polyamide and N-containing insoluble polymers.<sup>51–53</sup> Experimental results displayed in Figure 6 were in complete agreement with the expected structure: (i)  $^{13}\text{C}$  NMR spectra displayed the two signals assigned to the quaternary carbons belonging to the triazole ring (150.7 and 143.1 ppm), two lines for methylene (52.5 ppm) and methine (38.1 ppm) aliphatic carbons of the main chain, and a well-defined small peak at 173 ppm attributed to the carbonyl groups from MBA. The corresponding integration represented roughly 4% of the integration of triazole ring carbons. Although it does not represent a quantitative measure of the cross-linking level, this value reveals an efficient integration of MBA in the structure. (ii) In the  $^{15}\text{N}$  NMR spectra, we observed the three nitrogen atoms from the triazole ring (−94, −131, and −159 ppm). The use of the adiabatic sequence for the CP transfer enabled the detection of the small contribution from MBA (−254 ppm). The entire MAS  $^1\text{H}$  NMR spectrum acquired after a standard  $90^\circ$  (not shown) contained three contributions: a background resulting from the probe signal, a MAS modulated spectrum composed of wide lines (central band and spinning sidebands), with narrower peaks only on the central band.

The central part of the  $^1\text{H}$  NMR spectrum recorded by the CPMG pulse train filter is presented in Figure 7. It contains two very narrow peaks at 0.9, 1, and 3.5 ppm and two broader ones at 8.1 and 4.4 ppm. The corresponding  $T_2$  relaxation times measured with the 2D CPMG experiment are also given in Figure 7.

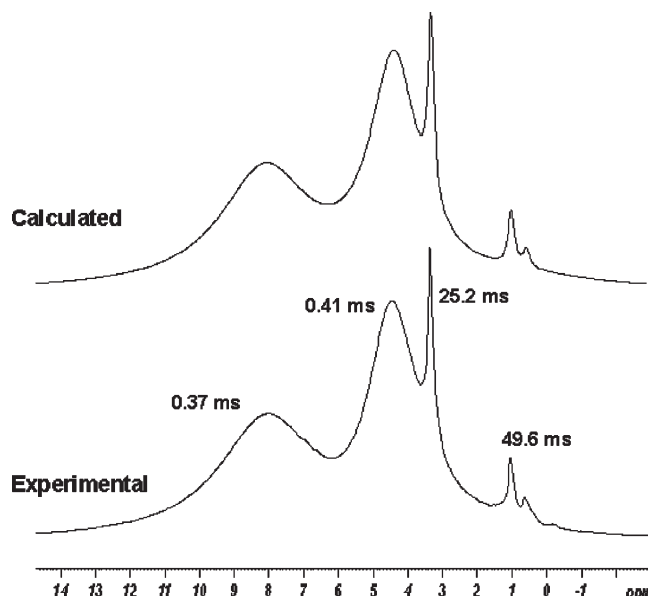


**Figure 7.**  $^1\text{H}$  MAS NMR spectrum obtained at 15 kHz with the CPMG sequence (with  $n = 2$ ) and calculated spectrum.  $T_2$  relaxation times of each line measured by the 2D CPMG sequence are also given in ms.

The broad component at 4.4 ppm was assigned to water and most of the narrow lines to free ethanol, since this solvent was utilized in the process. The assignment was confirmed by recording spectra under the same experimental conditions but after addition of a small quantity of water and ethanol to the sample.

The CPMG experiment was performed two times for quantitative analysis: with a number of cycles  $n = 2$  (that corresponds to a total relaxation delay of 0.53 ms) to measure the intensity of the broad components and  $n = 4$  for the narrower components (twice the relaxation delay). The different components in the proton spectrum were resolved by deconvolution, and the determined amplitudes were thus corrected according to their respective  $T_2$  relaxation time to account for signal loss during the total relaxation delay.

Finally, these values together with the integrations of the entire spectrum and of the probe signal contribution determined independently were used for quantitative analysis. The calculation yielded a water mass fraction of 9% and only a small ethanol mass contribution close to 0.2%. To ascertain this result, TGA measurements were performed on the same sample without any prior thermal treatment. A mass loss of 9% was also observed around 100  $^\circ\text{C}$  on the thermogram, confirming the highly hygroscopic nature of the compound.

An examination of the NMR spectral line characteristics provided information on the dynamics and localization of water. First, the rather short  $T_2$  value was compatible with bonded water. Second, it should be noticed that this line and the other broad line at 8.1 ppm, corresponding to triazole protons, demonstrated similar  $T_2$  relaxation times. This similarity suggests that both molecular entities experienced the same dynamics. Moreover, the corrected integrations were almost identical indicating that, on average, one water molecule was associated with one triazole, with both groups bearing two protons. A comparison of the entire spectrum integration demonstrated that about 50% of the triazole groups were linked to water molecules. This result



is actually consistent with the substantial solubility of poly(1-vinyl-1,2,4-triazole) in water,<sup>1</sup> which has been attributed to the hydrogen bond formation with the basic nitrogen atoms of pyridine type.<sup>46</sup>

## CONCLUSIONS

This article describes the preparation of polyHIPE materials based on 1-vinyl-1,2,4-triazole copolymerized with *N,N'*-methylenebis(acrylamide) as the cross-linker that are among the only few heterocycle-containing polyHIPEs described. The obtained monoliths presented the expected open-cell morphology and exhibited an unusually high mechanical strength to compression for nonreinforced polyHIPE materials. For example, a VT-MBA polyHIPE with an experimental porosity of about 87%, an average connection size of 1.8  $\mu\text{m}$ , and an average cell size of  $6.5 \pm 0.5 \mu\text{m}$  possessed a compressive Young's modulus of  $\sim 21$  MPa. A comprehensive high-resolution solid-state NMR study has been conducted on these materials that comfort the existence of water association between polytriazole chains. This kind of material is susceptible to being used in various applications such as reactive hyperporous polymers in catalyst supports or in green chemistry applications.

## AUTHOR INFORMATION

### Corresponding Authors

\*E-mail: h.deleuze@ism.u-bordeaux1.fr (H.D.); pascal.palmas@cea.fr (P.P.).

## ACKNOWLEDGMENT

The Commissariat à l'Énergie Atomique et aux Énergies Alternatives (CEA) is gratefully acknowledged for partial financial support (to F.A.).

## REFERENCES

- (1) For a recent review see: Kizhnyayev, V. N.; Pokatilov, F. A.; Vereshchagin, L. I. *Polym. Sci., Ser. C* **2008**, *50*, 1–21 (translation from *Vysokomol. Soedin., Ser. C* **2008**, *50*, 1296–1321).
- (2) Tatarova, L. A.; Ermakova, T. G.; Berlin, A. A.; Razvodovskii, E. F.; Lopyrev, V. A.; Kedrina, N. F.; Enikolopyan, N. S. *Vysokomol. Soedin., Ser. A* **1982**, *24*, 2205–2210 (CAN 98:17097).
- (3) Tatarova, L. A.; Morosova, I. S.; Ermakova, T. G.; Lopyrev, V. A.; Kedrina, N. F.; Enikolopyan, N. S. *Vysokomol. Soedin., Ser. A* **1983**, *25*, 14–17 (CAN 98:107839).
- (4) Ermakova, T. G.; Kuznetsova, N. P.; Maksimova, K. A. *Russ. J. Appl. Chem.* **2003**, *76*, 1971–1973 (translation from *Zh. Prikl. Khim.* **2003**, *76*, 2022–2024).
- (5) Izvozchikova, V. A.; Zakharova, O. G.; Voskoboinik, G. A.; Semchikov, Y. D. *Russ. J. Appl. Chem.* **2003**, *76*, 431–433 (translation from *Zh. Prikl. Khim.* **2003**, *76*, 446–448).
- (6) Uzun, L.; Kara, A.; Tuzman, N.; Karabakan, A.; Besirli, N.; Denisl, A. *J. Appl. Polym. Sci.* **2006**, *102*, 4276–4283.
- (7) Ermakova, T. G.; Shaulina, L. P.; Kuznetsova, N. P.; Burova, O. A.; Amosova, S. V.; Myachina, G. F. *Russ. J. Appl. Chem.* **2008**, *81*, 285–289 (translation from *Zh. Prikl. Khim.* **2008**, *81*, 295–299).
- (8) Xue, H.; Gao, H.; Shreeve, J. M. *J. Polym. Sci., Part A: Polym. Chem.* **2008**, *46*, 2414–2421.
- (9) Barby, D.; Haq, Z. European Patent 60 138, March, 3, 1982.
- (10) Lissant, K. J. In *Emulsions and Emulsions Technology Part 1*; Marcel Dekker Inc.: New York, 1974.
- (11) Menner, A.; Powell, R.; Bismarck, A. *Macromolecules* **2006**, *39*, 2034–2035.
- (12) Cameron, N. R.; Sherrington, D. C. *Adv. Polym. Sci.* **1996**, *126*, 163–213.
- (13) Silverstein, M. S.; Tai, H. W.; Sergienko, A.; Lumelsky, Y. L.; Pavlovsky, S. *Polymer* **2005**, *46*, 6682–6694.
- (14) Bhumgara, Z. *Filtr. Sep.* **1995**, *32*, 245–251.
- (15) Akay, G.; Birch, M. A.; Bohkhar, M. A. *Biomaterials* **2004**, *25*, 3991–4000.
- (16) Krajnc, P.; Brown, J. F.; Cameron, N. R. *Org. Lett.* **2002**, *4*, 2497–2500.
- (17) Menner, A.; Ikem, V.; Salgueiro, M.; Shaffer, M. S. P.; Bismarck, A. *Chem. Commun.* **2007**, 4274–4276.
- (18) Lucchesi, C.; Pascual, S.; Dujardin, G.; Fontaine, L. *React. Funct. Polym.* **2008**, *68*, 97–102.
- (19) Williams, J. M.; Wroblewski, D. A. *Langmuir* **1988**, *4*, 656–662.
- (20) Williams, J. M.; Gray, A. J.; Wilkerson, M. H. *Langmuir* **1990**, *6*, 437–444.
- (21) Akay, G.; Bhumgara, Z.; Wakeman, R. J. *Chem. Eng. Res. Des.* **1995**, *73*, 782–797.
- (22) Barbetta, A.; Cameron, N. R.; Cooper, S. J. *Chem. Commun.* **2000**, 221–222.
- (23) Barbetta, A.; Cameron, N. R. *Macromolecules* **2004**, *37*, 3188–3201.
- (24) Barbetta, A.; Cameron, N. R. *Macromolecules* **2004**, *37*, 3202–3212.
- (25) Tai, H.; Sergienko, A.; Silverstein, M. S. *Polym. Eng. Sci.* **2001**, *41*, 1540–1552.
- (26) Lépine, O.; Birot, M.; Deleuze, H. J. *Polym. Sci., Part A: Polym. Chem.* **2007**, *45*, 4193–4203.
- (27) Normatov, J.; Silverstein, M. S. *Macromolecules* **2007**, *40*, 8329–8335.
- (28) Menner, A.; Powell, R.; Bismarck, A. *Soft Matter* **2006**, *4*, 337–342.
- (29) Leber, N.; Fay, J. D. B.; Cameron, N. R.; Krajnc, P. *J. Polym. Sci., Part A: Polym. Chem.* **2007**, *45*, 4043–4053.
- (30) Junkar, I.; Koloini, T.; Krajnc, P.; Nemec, D.; Podgornik, A.; Strancar, A. *J. Chromatogr., A* **2007**, *1144*, 48–54.
- (31) Krajnc, P.; Stefanec, D.; Pulko, I. *Macromol. Rapid Commun.* **2005**, *26*, 1289–1293.
- (32) Ko, Y. C.; Lindsay, J. D. World Patent 044 041, May 27, 2004.
- (33) Barbetta, A.; Dentini, M.; Zannoni, E. M.; De Stefano, M. *Langmuir* **2005**, *21*, 12333–12341.
- (34) Barbetta, A.; Dentini, M.; De Vecchi, M. S.; Filippini, P.; Formisano, G.; Caiazza, S. *Adv. Funct. Mater.* **2005**, *15*, 118–124.
- (35) Duke, J. R.; Hoisington, M. A.; Langlois, D. A.; Benicewicz, B. C. *Polymer* **1998**, *39*, 4369–4378.
- (36) Cameron, N. R.; Sherrington, D. C. *Macromolecules* **1997**, *30*, 5860–5869.
- (37) Audouin, F.; Birot, M.; Pasquinet, E.; Deleuze, H.; Besnard, O.; Poullain, D. *J. Appl. Polym. Sci.* **2008**, *108*, 2808–2813.
- (38) Youssef, C.; Backov, R.; Treguer, M.; Birot, M.; Deleuze, H. *J. Polym. Sci., Part A* **2010**, *48*, 2942–2997.
- (39) Besnard, O.; Pasquinet, E.; Birot, M.; Deleuze, H.; Audouin, F. World Patent 15 0113 (A1), Dec 19, 2009.
- (40) Lépine, O.; Birot, M.; Deleuze, H. *Colloid Polym. Sci.* **2008**, *286*, 1273–1280.
- (41) Hediger, S.; Meier, B. H.; Ernst, R. R. *Chem. Phys. Lett.* **1995**, *240*, 449–456.
- (42) Brunauer, S.; Emmett, P. H.; Teller, E. *J. Am. Chem. Soc.* **1938**, *60*, 309–319.
- (43) Menner, A.; Salgueiro, M.; Shaffer, M. S. P.; Bismarck, A. *J. Polym. Sci., Part A: Polym. Chem.* **2008**, *46*, 5708–5714.
- (44) Lopyrev, V. A.; Salaurov, V. N.; Kurochkin, V. N.; Tatarova, L. A.; Ermakova, T. G. *Vysokomol. Soedin., Ser. B* **1985**, *27*, 145–151 (CAN 102:167297).
- (45) Ermakova, T. G.; Kuznetsova, N. P.; Tatarova, L. A.; Lopyrev, V. A. *Russ. J. Gen. Chem.* **2007**, *77*, 132–134 (translation from *Zh. Obsh. Khim.* **2007**, *77*, 141–143).

- (46) Mabile, C.; Leal-Calderon, F.; Bibette, J.; Schmitt, V. *Europhys. Lett.* **2003**, *5*, 708–714.
- (47) Schmitt, V.; Leal-Calderon, F.; Bibette, J. *Top. Curr. Chem.* **2003**, *227*, 195–215.
- (48) Gilson, L. J.; Ashby, M. F. *Cellular Solids*, 2nd ed.; Cambridge University Press: Cambridge, 1997; pp 175–189.
- (49) Mercier, A.; Kuroki, S.; Ando, I.; Deleuze, H.; Mondain-Monval, O. *J. Polym. Sci., Polym. Phys.* **2001**, *39*, 956–963.
- (50) Cummins, D.; Duxbury, C. J.; Quaedflieg, P. J. L. M.; Magusin, P. C. M. M.; Koning, C. E.; Heise, A. *Soft Matter* **2009**, *5*, 804–811.
- (51) Asano, A.; Nishioka, M.; Takahashi, Y.; Kato, A.; Hikasa, S.; Iwabuki, H.; Nagata, K.; Sato, H.; Hasegawa, T.; Sawabe, H.; Arao, M.; Suda, T.; Isoda, A.; Mukai, M.; Ishikawa, D.; Izumi, I. *Macromolecules* **2009**, *42*, 9506–9514.
- (52) Vanhaecht, B.; Goderis, B.; Magusin, P. C. M. M.; Mezari, B.; Dolbnya, I.; Koning, C. E. *Macromolecules* **2005**, *38*, 6048–6055.
- (53) Feng, Y.; Schmidt, A.; Weiss, R. A. *Macromolecules* **1996**, *29*, 3909–3917.